Assessment of Diffuse Optical Tomography Image Reconstruction Methods Using a Photon Transport Model

M. M. Althobaiti[1], H. S. Salehi[2], Q. Zhu[2]

[1]Department of Biomedical Engineering, University of Connecticut, Storrs, CT, USA

[2]Department of Electrical and Computer Engineering, University of Connecticut, Storrs, CT, USA

Abstract

INTRODUCTION: Imaging of tissue with near-infrared diffuse optical tomography is emerging as a practical method to map hemoglobin concentrations within tissue for breast cancer detection and diagnosis. The accurate recovery of images by using numerical modeling requires an effective image reconstruction method. We illustrate a comparison between two widely used reconstruction methods using finite element modeling in COMSOL Multiphysics® software for 3D forward data generation. The first reconstruction method was born approximation [1,2], which was developed in our laboratory. The second method was an image reconstruction package "NIRFAST" that was developed at Dartmouth College [3,4]. The image reconstruction assessments were performed based on various tumor sizes, depths, and absorption coefficients. Simulation studies demonstrated the capability of each reconstruction method to recover the true values of absorption coefficients.
USE OF COMSOL MULTIPHYSICS: A 3D model was defined in COMSOL Multiphysics using Helmholtz Equation [5] with proper boundary conditions, subdomains, and mesh size as shown in Fig. 1. Nine light sources and fourteen optical detectors were utilized to estimate the fluence. The extracted fluence from our COMSOL model was employed to map the absorption coefficient using image reconstruction methods.
RESULTS: The results indicate that both methods provide similar performances for detecting large tumor sizes, and maximum reconstructed value was more than 60% of the true value. However, for small tumor sizes, born approximation method provided higher reconstructed values of absorption coefficient, consequently, better tumor detection as shown in Fig. 2. Additionally, when we simulated the same tumor size with different depths, results indicated that both methods provide good tumor contrast at shallow depths. For tumors deeply positioned in breast, the maximum reconstructed absorption coefficient was low for both methods and results for both methods were similar. It can be seen from Figs. 3 and 4, artifacts surrounding the target was the case for all NIRFAST reconstructed images. Furthermore, we expect to have similar results when tumors with different absorption coefficients were simulated.
CONCLUSION: The performance of two image reconstruction methods for near-infrared diffuse optical tomography was investigated. For future, this model could also be used to study the effect of adding the chest wall layer on reconstructed images. It also could be used to study the

different type's breast tumors.

Reference

1. Q. Zhu, C. Xu, PY. Guo, A. Aquirre, B. Yuan, F. Huang, D. Castilo, J. Gamelin, S. Tannenbaum, M. Kane, P. Hedge, and S. Kurtzman, Optimal probing of optical contrast of breast lesions of different size located at different depths by US localization, Technology in Cancer Research & Treatment 5(4), 365-380 (August 2006)

2. M. Huang and Q. Zhu, A Dual-mesh optical tomography reconstruction method with depth correction using a priori ultrasound information, Applied Optics 43(8), 1654-1662 (2004)

3. M. Jermyn, H. Ghadyani, M.A. Mastanduno, W. Turner, S.C. Davis, H. Dehghani, and B.W. Pogue, Fast segmentation and high-quality three-dimensional volume mesh creation from medical images for diffuse optical tomography, Journal of Biomedical Optics. 18 (8), 086007 (August 12, 2013)

4. H. Dehghani, M.E. Eames, P.K. Yalavarthy, S.C. Davis, S. Srinivasan, C.M. Carpenter, B.W. Pogue, and K.D. Paulsen, Near infrared optical tomography using NIRFAST: Algorithm for numerical model and image reconstruction, Communications in Numerical Methods in Engineering, Vol. 25, 711-732 (2009)

5. L. V. Wang and H.-i Wu, Biomedical Optics: Principles and Imaging (Wiley, 2007).

Figures used in the abstract

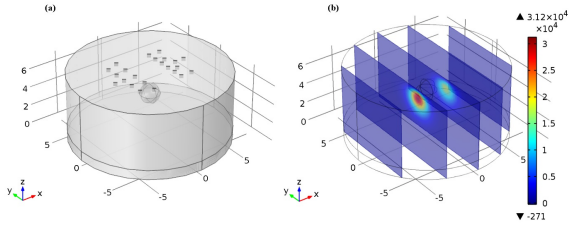

Figure 1: (a) Geometry including the placements of sources and detecters (9 sources and 14 detecters) on the top layer. (b) The simulated flouance of only one source.

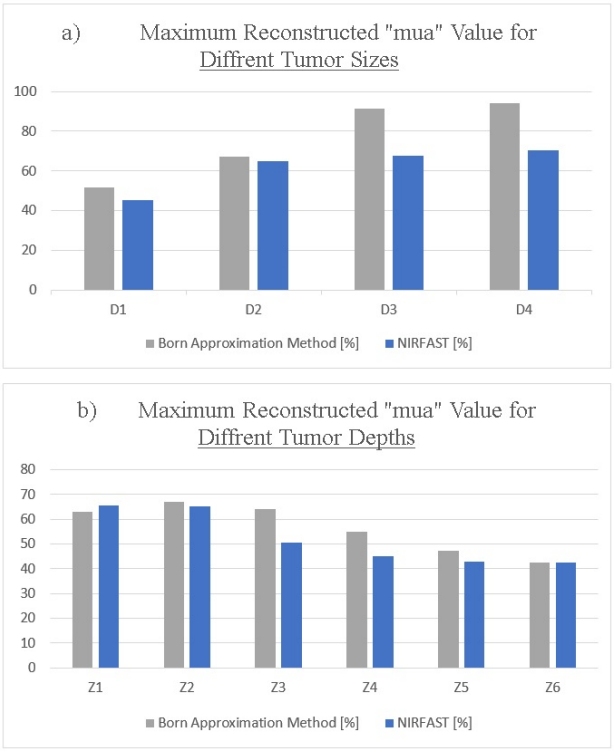

Figure 2: Percentage of the maximum reconstructed "mua" value to the true value, 0.2 cm-1. For (a) different target sizes. (b) different target depths.

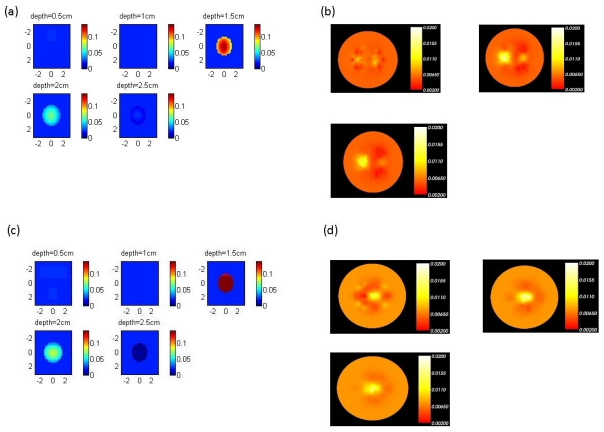

Figure 3: DOT reconstruction using two methods Born Approximation, (a) and (c), and NIRFAST, (b) and (d). Both are for the same target depth (2cm): the first row corresponds to a target (tumor) of 1.5 cm diameter. The second row corresponds to a target (tumor) of 2.5 cm diameter.

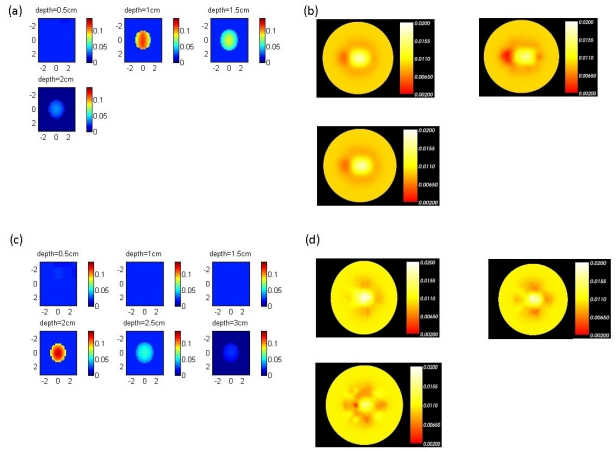

Figure 4: DOT reconstruction using two methods Born Approximation, (a) and (c), and NIRFAST, (b) and (d). Both are for the same target size (diameter=2cm): the first row corresponds to a target (tumor) of 2 cm depth. The second row corresponds to a target (tumor) of 2.5 cm depth.